ACS OMEGA

http://pubs.acs.org/journal/acsodf

Article

Parameter Optimization of Asynchronous Cyclic Waterflooding for Horizontal−Vertical Well Patterns in Tight Oil Reservoirs

Shaofei Kang, Chunsheng Pu,* Yuchuan Wang, Wei Liu, Kai Wang, Feifei Huang, Qiao Fan, Xiang Gao, and Qiangqiang Yang

Cite This: *ACS Omega* 2022, 7, 11226−11239

Read Online

ACCESS | Metrics & More | Article Recommendations

ABSTRACT: Tight oil resources in China are mainly exploited by staged-fractured horizontal wells; horizontal wells face the problems of the rapid decline rate and low primary oil recovery. Pilot tests on the asynchronous cyclic waterflooding for the horizontal−vertical well pattern were carried out in recent years and achieved good performance. However, there are few studies on the influencing factors and parameter optimization of asynchronous cyclic waterflooding, which limits its wide application. This work took the tight oil reservoir in Yanchang formation, Fuxian area, Ordos Basin as its object, and the oil recovery mechanisms of asynchronous cyclic waterflooding for the horizontal−vertical well pattern were analyzed first. Then, the operation parameters of asynchronous cyclic waterflooding were optimized by the numerical simulation method. Among them, the injection proportion was optimized by the fuzzy synthetic evaluation method. Finally, the oilfield test was carried out based on the optimized parameters. The results showed that pressure disturbance and streamline deviation are the main oil recovery mechanisms of asynchronous cyclic waterflooding. The asynchronous mode of the diagonal well row is better than other asynchronous modes. For the injection time interval, injection−production ratio, and the injection and shut-in time, the cumulative oil production all show the trend of increasing first and then decreasing with the increase in these parameters. The optimal injection time interval and injection−production ratio are 0.5 T and 1, respectively. The optimal injection and shut-in time can be calculated by empirical formulas. Ultimately, the fuzzy synthetic evaluation model was established to optimize the injection proportion. Field practices showed that the average daily oil production of horizontal wells was increased from 1.7 to 3.0 m^3 with the optimized parameters, which further verified the accuracy of the optimized parameters. This research can provide theoretical support for the effective development of tight oil reservoirs.

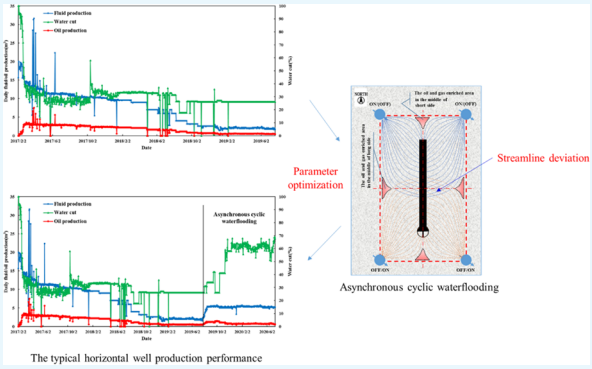

1. INTRODUCTION

Given the rapid depletion of conventional oil production and the rising energy demand, tight oil reservoirs play a significantly important role in the development of oil and gas fields for their abundant geological reserves.[1−3] Tight oil resources in China are rich, with a geological reserve estimation of 178.2×10^8 t, which is mainly distributed in the Ordos Basin, Tarim Basin, Sichuan Basin, Songliao Basin, Bohai Basin, and Jungar Basin.[4−7] The staged-fracturing horizontal well technology is an effective method for the development of tight oil reservoirs.[8−12] However, the oil production of horizontal wells declines rapidly within the first few years, and the oil recovery during the primary depletion period is usually less than 10%.[13−15] Effective energy supplementation methods have become an important topic for maintaining the production rate of horizontal wells. Water huff-n-puff technology and waterflooding technology are the common energy supplementation methods for horizontal wells currently.[16−22] However, for the horizontal−vertical well patterns, the horizontal wells are not in the isolated formation units, which makes it difficult to hold the formation pressure during the huff-n-puff. Therefore, the ultimate recovery is low. Previous studies have shown that waterflooding exhibits a better performance on the formation energy maintenance for the horizontal−vertical well pattern.[23,24] In recent years, pilot tests of the development mode with vertical wells injection and horizontal wells production in the horizontal−vertical well pattern have been applied in several oil fields, and most of the cases are successful. Clearly, for the horizontal−vertical well pattern, the development mode with vertical well injection and

Received: January 6, 2022
Accepted: March 11, 2022
Published: March 22, 2022

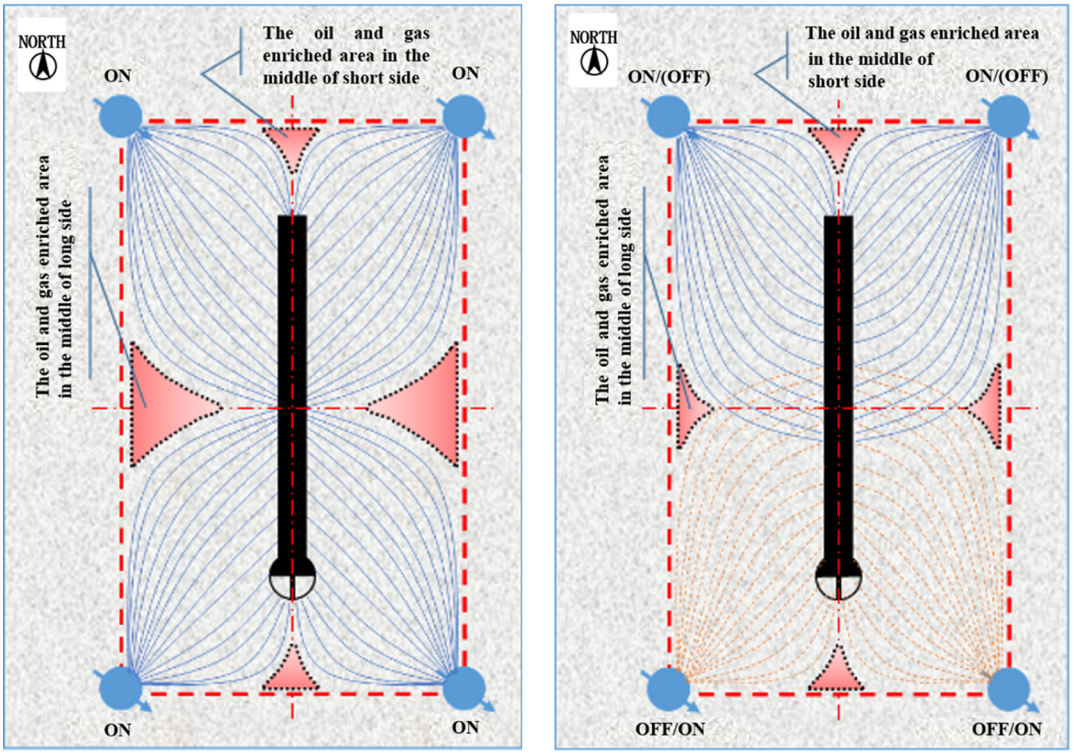

(a) (b)

Figure 1. Swept area of different injection modes: (a) synchronous cyclic waterflooding and (b) asynchronous cyclic waterflooding.

horizontal well production has become a promising approach for enhanced oil recovery of horizontal wells. The tight oil reservoir in the Fuxian area is located in the southeast of the Ordos Basin, NW China, with developed natural micro-fractures. In addition, the fracture network of horizontal wells is large, and the well spacing between vertical well and horizontal well is small; therefore, the waterflooding method could exhibit better performance on the formation energy maintenance for the horizontal–vertical well in the tight oil reservoirs in the Fuxian area. However, there are few studies on the influencing factors of waterflooding for the horizontal–vertical well pattern, which results in a huge difference in the production performance of horizontal wells.

Currently, a lot of research has been carried out on the seepage characteristics of the horizontal well in the horizontal–vertical well pattern. Lang and Wang et al. studied the seepage law of the horizontal well in the five-spot and seven-spot horizontal–vertical well patterns and further deduced the mathematical expressions of horizontal well production, sweep efficiency, and flow function.[25−27] Subsequently, using the seepage resistance method, Wu et al. investigated the water breakthrough time of horizontal well in the horizontal–vertical well pattern in 2005.[28] Results indicated that the length of horizontal wells has a significant influence on the water breakthrough time of horizontal wells. Moreover, compared with the seven-spot and inverted nine-spot horizontal–vertical well patterns, the horizontal well in the five-spot horizontal–vertical well pattern has the latest water breakthrough time. Moreover, using the numerical simulation method, Wu et al. also investigated the influence of the angle between the horizontal well and the horizontal direction on the sweep efficiency of the waterflooding in the horizontal–vertical well patterns.[29] They found that the sweep efficiency of the waterflooding in the five-spot horizontal–vertical well pattern decreases with the increase in the angle but increases in the seven-spot and nine-spot horizontal–vertical well pattern. However, during the waterflooding, the large scale of the fracture networks formed by hydraulic fracturing is easy to lead to water channeling in horizontal wells. Research and field practices indicated that cyclic waterflooding can bring into full play the effect of pressure disturbance, making the injected water streamline sweep over the remaining oil area which is difficult to be swept by conventional waterflooding, improving the sweep efficiency of waterflooding, and thus delaying the water breakthrough time of horizontal well.[30−32] Cyclic waterflooding is a waterflooding method proposed by the scholar of the Soviet Union in the late 1950s and early 1960s, which can improve the development effect of waterflooding by changing the injection rate periodically.[33] The pressure disturbance is the main oil recovery mechanism of cyclic waterflooding. It could promote the fluid exchange between the fracture (high-permeability areas) and matrix (low-permeability areas) in the fractured reservoir, making the displacement of injected water uniform relatively, avoiding further increment of water cut, thus delaying the water breakthrough time of wells.[34−36] Many studies have been carried out on the oil recovery mechanism and influencing factors of cyclic waterflooding. However, there are few studies on parameter optimization of cyclic waterflooding, and most of these studies focused on the qualitative study of parameter optimization. Previous studies indicated that the development effect of the asymmetric cyclic waterflooding mode with short injection time and long shut-in time is the best compared with other symmetrical cyclic waterflooding modes.[37,38] Water channeling is not easy to occur during the asymmetric cyclic

https://doi.org/10.1021/acsomega.2c00097
ACS Omega 2022, 7, 11226−11239

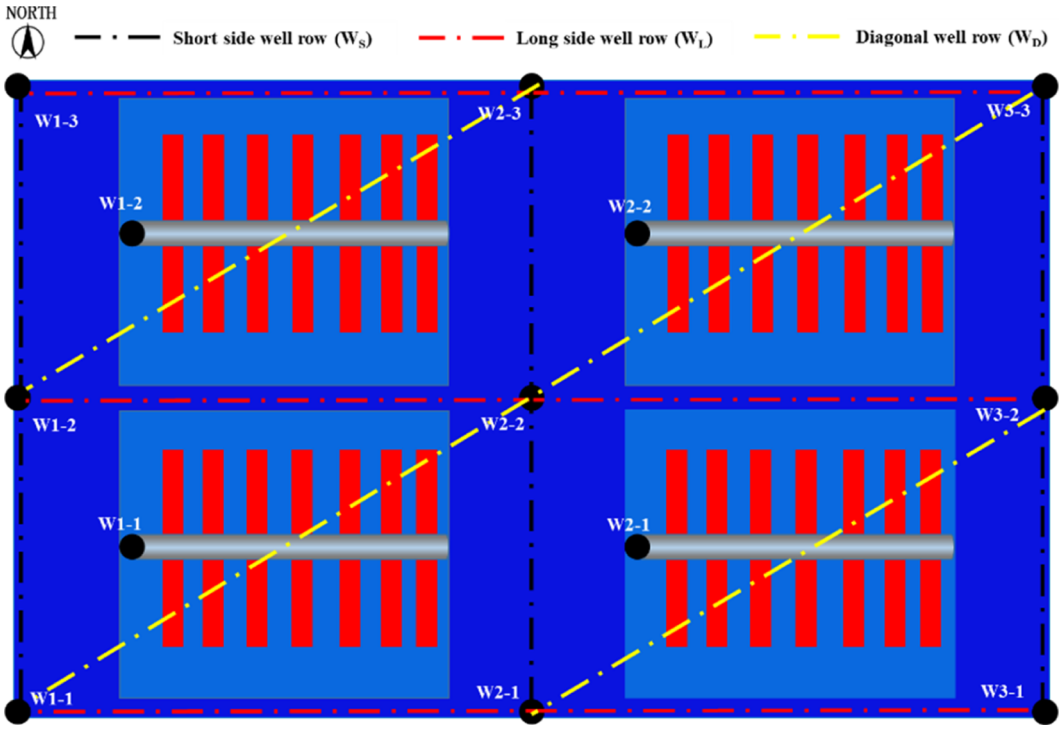

Figure 2. Reservoir model includes four inverted five-spot horizontal−vertical well patterns.

waterflooding with short injection time and long shut-in time, which leads to the higher ultimate oil recovery. Besides, they found that high injection pressure is also beneficial for pressure maintenance during the injection stage. In 2018, Sun et al. proposed a simulated annealing genetic algorithm to optimize the process parameter based on the identification of water channeling.[39] Results further verified that asymmetric cyclic waterflooding exhibits a better performance on the formation energy supplementation in the horizontal−vertical well pattern than symmetric cyclic waterflooding. In the same year, Kobra Pourabdollah used the real-time monitoring data of cyclic waterflooding to optimize the injection time and shut-in time of cyclic waterflooding based on the dual-porosity generalized component model.[40] However, to the best of our knowledge, very limited research on parameter optimization of asynchronous cyclic waterflooding for the horizontal−vertical well pattern is available currently.

Taking the tight oil reservoir in Yanchang formation of Fuxian area in the southeast of the Ordos Basin, parameter optimization of asynchronous cyclic waterflooding for the horizontal−vertical well pattern was investigated by the numerical simulation method. First, oil recovery mechanisms of asynchronous cyclic waterflooding for the horizontal−vertical well pattern were analyzed. Then, operation parameters of asynchronous cyclic waterflooding, including the asynchronous mode, the injection time interval, the injection and shut-in time, and the injection−production ratio, were optimized. Subsequently, the influence of the injection well position on the production performance of the horizontal well was investigated, and the control area of the injection well was calculated. On this basis, the injection proportion was optimized by the fuzzy synthetic evaluation method. Finally, field practice was carried out based on the optimized parameters. This work can provide some guidance to the field application of asynchronous cyclic waterflooding for the horizontal−vertical well pattern.

2. OIL RECOVERY MECHANISMS OF ASYNCHRONOUS CYCLIC WATERFLOODING FOR THE HORIZONTAL−VERTICAL WELL PATTERN

The pressure disturbance is the main oil recovery mechanism of cyclic waterflooding for fractured reservoirs.[32] In the cyclic waterflooding process, water is injected into the formation periodically, and the pressure disturbance is caused by the difference in pressure transmitting coefficients in high and low permeability areas, which accelerates the fluid exchange between high the low permeability areas, enhances the capillary imbibition efficiency, thus improving the sweep efficiency and oil displacement efficiency. Besides, part of the oil phase can overcome the Jamin effect and flow across the narrow throat due to the presence of pressure difference, which further improves the ultimate recovery of the remaining oil.[41,42] Figure 1 shows the swept area of synchronous and asynchronous cyclic waterflooding. From Figure 1, the oil and gas enriched area in the middle of the short and long side of the horizontal−vertical well pattern for asynchronous cyclic waterflooding are both much smaller than that for synchronous cyclic waterflooding. The reason is that the streamline deviation caused by the asynchronous injection of injection wells further enlarges the swept area of injected water. From the analysis above, the pressure disturbance and the streamline deviation are the main oil recovery mechanisms of asynchronous cyclic waterflooding in the horizontal−vertical well pattern.

3. METHODOLOGY

Compared with the inverted seven-spot and inverted nine-spot horizontal−vertical well pattern, the water breakthrough happens late in the inverted five-spot horizontal−vertical well pattern, which means the best production performance of horizontal wells.[28] Therefore, by establishing the inverted five-spot horizontal−vertical well pattern reservoir model, the operating parameters, including asynchronous mode, injection

https://doi.org/10.1021/acsomega.2c00097
ACS Omega 2022, 7, 11226−11239

and shut-in time, injection time interval, injection proportion, and injection−production ratio, were optimized. The reservoir model includes four horizontal−vertical well patterns, as shown in Figure 2. The fracture number in each horizontal well is 7, fracture half-length is 250 m, and the fracture network width is 20 m. Parameters used in this model were obtained from the tight oil reservoir in the Yanchang formation of the Fuxian area and are summarized in Table 1.

Table 1. Reservoir and Fracture Properties

name	value
length of the horizontal well, m	225
initial reservoir pressure, MPa	11.3
reservoir temperature, °C	54
porosity, fraction	0.08
average permeability in non-fracturing area, mD	0.17
average permeability of the main fracture in fracturing area, mD	200
average permeability of secondary fracture in fracturing area, mD	23
width of the fracture network, m	20
half-length of fracture, m	250

4. RESULTS AND DISCUSSION

4.1. Asynchronous Mode and the Injection Time Interval. The asynchronous mode and the injection time interval have a very large impact on the performance of asynchronous cyclic waterflooding for the horizontal−vertical well pattern from time and space, respectively. The asynchronous mode can be defined as the asynchronous injection of well rows in different directions. It can be divided into three categories for inverted five-spot horizontal−vertical well pattern: the asynchronous mode of the short side well row (W_{AS}), the asynchronous mode of the long side well row (W_{AL}), and the asynchronous mode of the diagonal well row (W_{AD}), as shown in Figure 2. Moreover, the injection time interval (t) can be characterized by the overlap time of the injection period between adjacent well rows. To facilitate our understanding, the reservoir model is characterized by the matrix in the first column of Table 2, and W in the matrix represents the injection well. A series of simulations were conducted using different asynchronous modes (W_{AS}, W_{AL}, and W_{AD}) and injection time intervals ($a = 0.25T$, $b = 0.5T$, $c = 0.75T$, and $d = T$). As shown in Table 2, the third column represents the start time of injection in the nth cycle for each well, where t_0, t, and T are the start time of injection in the first cycle, the injection time interval, and the injection period, respectively. For example, for the asynchronous mode of the short side well row (W_{AS}), in the first cycle ($n = 1$), the start time of injection for the wells (W_{1-1}, W_{1-2}, W_{1-3}, W_{3-1}, W_{3-2}, and W_{3-3}) are all t_0, and that for the wells (W_{2-1}, W_{2-2}, and W_{2-3}) are all $t_0 + t$. From the analysis above, we could define each scheme. In these cases,20 cycles were simulated.

The cumulative oil production at the end of 20 cycles of different schemes is shown in Figure 3. It can be seen from Figure 3 that the cumulative oil production increases first and then declines with the increase in injection time interval, and the scheme with 0.5 T showed the best effect. The reason is that when the injection time interval is small, the scheme is similar to the cyclic waterflooding, so the swept area is small, the cumulative oil production is low. The streamline deviation takes effect gradually with the increase in injection time interval, which results in the increase in swept area and the increase in cumulative oil production. When the injection time interval increase beyond 0.5 T, oil near the wellbore is displaced to the shut-in well row, which weakens the waterflooding effect of the shut-in well row and ultimately reduces the cumulative oil production. For the asynchronous mode, the degree to which the asynchronous mode affects the performance of asynchronous cyclic waterflooding can be concluded as follows: $W_{AD} > W_{AS} > W_{AL}$. For the asynchronous mode of the long side well row, because of the short distance between adjacent well rows, streamline interference occurs early, which weakens the streamline deviation effect, thus decreasing the swept area and reducing the cumulative oil production. Conversely, streamline interference occurs late for the asynchronous mode of the short side well row, which enhances the streamline deviation effect and increases the cumulative oil production. Besides, for the asynchronous mode of the diagonal well row, there are streamline deviations in the both short and long sides of the horizontal−vertical well pattern, which further increases the swept area. Therefore, the scheme with the asynchronous mode of the diagonal well row achieves the best production performance. The study in this section indicates that the optimal asynchronous mode and injection time interval are the asynchronous mode of the diagonal well row and 0.5T, respectively.

4.2. Injection and Shut-In Time. The injection and shut-in time have a significant influence on the redistribution of oil and water between the high and low permeability areas, thus affecting the production performance of asynchronous cyclic waterflooding. The optimal injection time and shut-in time

Table 2. Schemes with Different Asynchronous Modes and Injection Time Intervals

matrix characterization of injection wells in the five-spot well pattern	asynchronous mode	start time of injection in the nth cycle
$\begin{bmatrix} W_{1-1} & W_{1-2} & W_{1-3} \\ W_{2-1} & W_{2-2} & W_{2-3} \\ W_{3-1} & W_{3-2} & W_{3-3} \end{bmatrix}$	W_{AS}	$\begin{bmatrix} t_o + (n-1)T & t_o + (n-1)T & t_o + (n-1)T \\ t_o + t + (n-1)T & t_o + t + (n-1)T & t_o + t + (n-1)T \\ t_o + (n-1)T & t_o + (n-1)T & t_o + (n-1)T \end{bmatrix}$
	W_{AL}	$\begin{bmatrix} t_o + (n-1)T & t_o + t + (n-1)T & t_o + (n-1)T \\ t_o + (n-1)T & t_o + t + (n-1)T & t_o + (n-1)T \\ t_o + (n-1)T & t_o + t + (n-1)T & t_o + (n-1)T \end{bmatrix}$
	W_{AD}	$\begin{bmatrix} t_o + (n-1)T & t_o + t + (n-1)T & t_o + (n-1)T \\ t_o + t + (n-1)T & t_o + (n-1)T & t_o + t + (n-1)T \\ t_o + (n-1)T & t_o + t + (n-1)T & t_o + (n-1)T \end{bmatrix}$

https://doi.org/10.1021/acsomega.2c00097
ACS Omega 2022, 7, 11226−11239

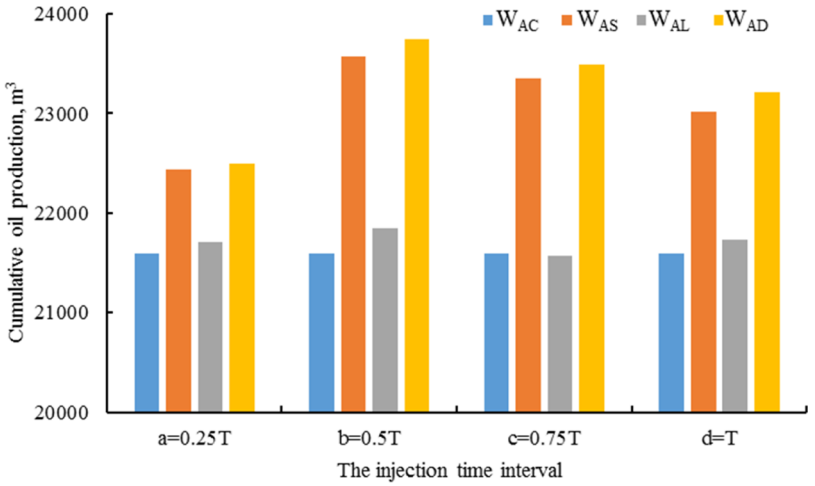

Figure 3. Cumulative oil production of horizontal wells with different asynchronous modes and injection time intervals.

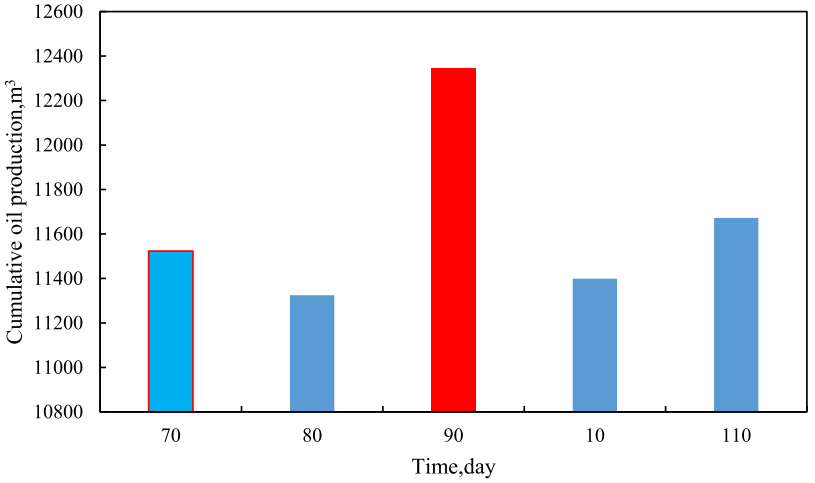

Figure 4. Horizontal well production performance of asynchronous cyclic waterflooding with different injection times and shut-in times.

should not only ensure the time needed for oil−water redistribution but also keep a certain pressure level to maintain the production rate for horizontal wells. Previous studies indicated that cyclic waterflooding achieves the best production performance when the injection time is the same as the shut-in time.[43] Therefore, to investigate the influence of injection and shut-in time on the performance of asynchronous cyclic waterflooding, a series of schemes with different injection and shut-in times of 70, 80, 90, 100, and 110 days were carried out, while keeping the injection volume as the same. As shown in Figure 4, the cumulative oil production at the end of 3000 days shows a trend of increasing first and then decreasing with the increase in injection and shut-in time, and the scheme with the injection and shut-in times of 90 days achieves the best production performance. The reason is that under the same injection volume, as the injection and shut-in time increase, the swept area increases due to the stable displacement front, so the cumulative oil production gets increased. However, with the further increase in injection and shut-in time, the streamline deviation is weakened and the swept area is decreased; thus, the cumulative oil production gets decreased. Therefore, there will be an optimal injection and shut-in time for the asynchronous cyclic waterflooding.

Currently, the injection time and shut-in time are mainly optimized by numerical simulation method and empirical method. According to previous studies, the injection time can be calculated using eq 1.[43] Based on the practical oilfield data of Chang8 formation in the Fuxian area of Yanchang oilfield, the injection time (T_1) can be determined as 92 days, which is close to the optimal injection time determined by numerical simulation results. Hence, eq 1 is suitable for the determination of injection time.

$$T_1 = \frac{L^2 c_t \phi \mu_o}{2K} \times \frac{1}{86{,}400} \quad (1)$$

where L is the average distance between the injection well and the horizontal well, cm; C_t is the formation comprehensive compressibility, 10^{-4} MPa^{-1}; K is the area-weighted average permeability, mD; μ_o is the underground viscosity of crude oil, mpa·s; T_1 is the injection time of the injection well, d; and φ is average porosity of rock, %.

4.3. Injection−Production Ratio. Taking into consideration of the great difference in the formation energy deficit degree in different horizontal−vertical well patterns, to better study the impact of the injection−production ratio on the performance of asynchronous cyclic waterflooding, a series of schemes with different injection−production ratios and formation energy deficit degrees have been designed, while keeping other parameters as the same, as shown in Table 3. In

https://doi.org/10.1021/acsomega.2c00097
ACS Omega 2022, 7, 11226−11239

Table 3. Simulation Schemes with Different Injection−Production Ratios and Formation Energy Deficit Degrees

group	the time of the natural energy development stage (day)	injection−production ratio
I	1000	(0.85, 0.9, 0.95, 1.0, 1.05, 1.1, 1.15, 1.2, 1.25, 1.3, 1.35, 1.4)
II	2000	
III	3000	
IV	4000	

this study, the time of the natural energy development stage is used to simulate the deficit degree of formation energy. The cumulative oil production at the end of 3000 days is used to evaluate the influence of the injection−production ratio on the performance of asynchronous cyclic waterflooding in different formation energy deficit degrees.

Figure 5 shows the cumulative oil production of asynchronous cyclic waterflooding with different deficit degrees of formation energy and injection−production ratios. From Figure 5, the short time of the natural energy development stage means the low formation energy deficit degree and the more remaining reserve. Therefore, with the decrease in the time of the natural energy development stage, the cumulative oil production of asynchronous cyclic waterflooding increases. In addition, the influence of the injection−production ratio on the performance of asynchronous cyclic waterflooding in different formation energy deficit degrees is the same. The cumulative oil production of asynchronous cyclic waterflooding first rises and then falls with the increase in the injection−production ratio and reaches the optimal value when the injection−production ratio is around 1. On the one hand, with the increase in the injection−production ratio, the pressure difference between the injection well and the production well increases, so the displacement rate increases, which enhances the streamline deviation effect and increases the swept area of injected water. Therefore, the cumulative oil production increases. On the other hand, with the increase in the injection−production ratio, the pressure fluctuation amplitude increases during the asynchronous cyclic waterflooding, which enhances the elastic drive effect and imbibition effect, so the cumulative oil production got further increased. However, with the further increase in the injection−production ratio, water channeling is easily caused due to the high-pressure difference between the injection wells and the production well, resulting in the increases of water cut of the production well. Moreover, water channeling could weaken the streamline deviation effect, decrease the swept area of injected water, thus leading to the decrease in cumulative oil production. Therefore, the optimal injection−production ratio for asynchronous cyclic waterflooding should be around 1.0.

4.4. Injection Proportion. *4.4.1. Influence of Injection Proportion on the Performance of Asynchronous Cyclic Waterflooding.* For the inverted five-spot horizontal−vertical well pattern, all the injection wells are the corner well, and each row has the same number of wells. Simulation results show that when the injection proportions of injection wells are the same, asynchronous cyclic waterflooding achieves the best production performance. It means the balanced injection mode is most favorable for asynchronous cyclic waterflooding in the inverted five-spot horizontal−vertical well pattern. However, there are corner wells and edge wells in the inverted seven-spot horizontal−vertical well pattern, so the influence of injection proportion on the performance of asynchronous cyclic waterflooding differs from that in the inverted five-spot horizontal−vertical well pattern. By establishing the inverted seven-spot

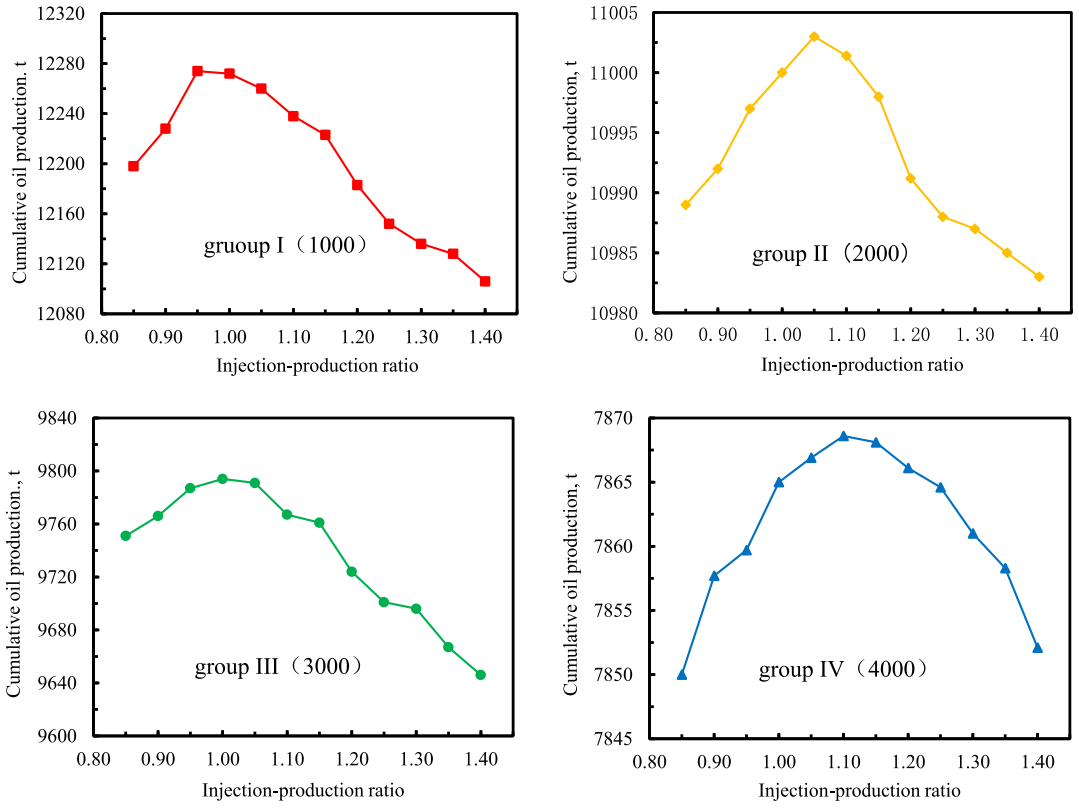

Figure 5. Cumulative oil production of asynchronous cyclic waterflooding at the different injection−production ratios.

https://doi.org/10.1021/acsomega.2c00097
ACS Omega 2022, 7, 11226−11239

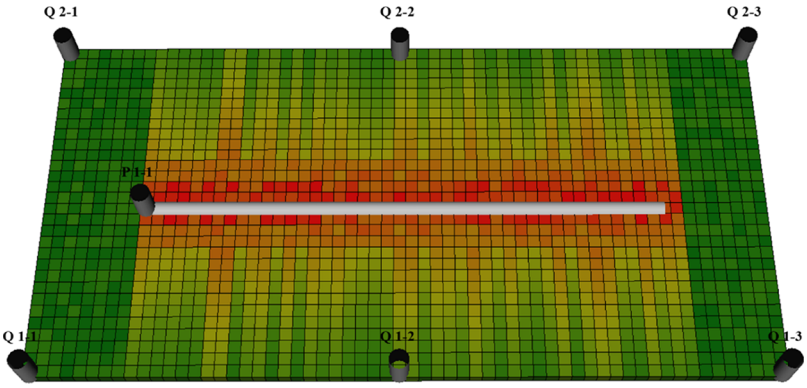

Figure 6. Reservoir model of the inverted seven-spot horizontal−vertical well pattern.

horizontal−vertical well pattern reservoir model, the influence of injection proportion on the performance of asynchronous cyclic waterflooding in the inverted seven-spot horizontal−vertical well pattern is studied. Based on parameters of the inverted five-spot horizontal−vertical well pattern reservoir model, the inverted seven-spot horizontal−vertical well pattern reservoir model is established, as shown in Figure 6, in which Q_{1-1}, Q_{1-3}, Q_{2-1}, and Q_{2-3} are corner wells, and Q_{1-2} and Q_{2-3} are edge wells.

Keeping the sum of injection proportion of injection wells in the inverted seven-spot horizontal-well pattern as 1, nine schemes are designed, as shown in Table 4. Those schemes can

Table 4. Schemes with Different Injection Proportions of Injection Wells in the Inverted Seven-Spot Horizontal−Vertical Well Pattern

	injection proportion of corner wells				injection proportion of edge wells	
scheme	Q_{1-1}	Q_{1-3}	Q_{2-1}	Q_{2-3}	Q_{1-2}	Q_{2-2}
QD-1	1/6	1/6	1/6	1/6	1/6	1/6
QD-2	0.18	0.18	0.18	0.18	0.14	0.14
QD-3	0.13	0.24	0.15	0.2	0.19	0.21
QD-4	0.17	0.17	0.17	0.17	0.16	0.16
QD-5	0.19	0.14	0.18	0.17	0.13	0.19
QD-6	0.16	0.16	0.16	0.16	0.18	0.18
QD-7	0.18	0.12	0.13	0.21	0.16	0.2
QD-8	0.15	0.15	0.15	0.15	0.2	0.2
QD-9	0.09	0.12	0.19	0.2	0.17	0.23

be divided into three categories according to the injection proportion of injection wells, which are the scheme of generally balanced injection proportion (QD-1), the scheme of classified balanced injection proportion (QD-2, QD-4, QD-6, and QD-8), and the scheme of casual injection proportion (QD-3, QD-5, QD-7, and QD-9). Those schemes are simulated while keeping other parameters the same.

Simulation results are standardized based on the cumulative oil production of the generally balanced injection scheme (QD-1), and the final results are shown in Figure 7. It can be seen from Figure 7 that compared with the generally balanced injection scheme and the casual injection proportion scheme, the classified balanced injection scheme (QD-4) achieves the best production performance. It means the classified balanced injection scheme is more beneficial to the asynchronous cyclic waterflooding. From the analysis above, the determination of injection proportion for asynchronous cyclic waterflooding can

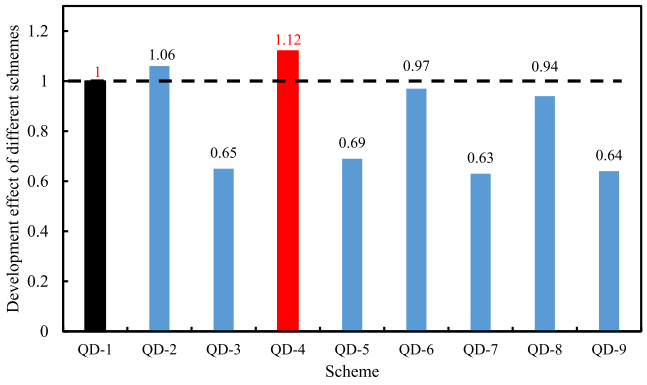

Figure 7. Cumulative oil production of asynchronous cyclic waterflooding for different schemes.

be concluded as follows: (1) if two injection wells are both centrosymmetric and axisymmetric about the horizontal well, the waterflooding effects of two wells are the same, so the injection proportions of two wells are the same. On the contrary, if two injection wells are neither centrosymmetric nor axisymmetric about the horizontal well, the injection proportions of the two wells are different. (2) The injection proportion of the corner wells is usually larger than that of the edge wells. However, there are fewer studies on the injection proportion optimization of the asynchronous cyclic waterflooding for the horizontal−vertical well pattern, so the optimization of injection proportion is particularly studied in this study.

4.4.2. Injection Proportion Optimization. Horizontal−vertical well patterns are not always regular, which further increases the difficulty of injection proportion optimization. The injection proportion is strongly influenced by the injection well position and the control area of the injection well. Hence, to optimize the injection proportion of injection wells in the horizontal−vertical well pattern, the influence of the injection well position on the horizontal well production performance in the horizontal−vertical pattern was investigated first. Then, the control area of the injection well was calculated. Finally, using the fuzzy comprehensive evaluation method, the injection proportion of injection wells could be determined.

4.4.2.1. Influence of Injection Well Position on the Horizontal Well Production Performance. Affected by fracturing area in horizontal wells, the impact of the injection well position on the horizontal well production performance in the horizontal−vertical pattern is nonlinear with the distance between them. Therefore, to accurately study the influence of the injection well position on the horizontal well production

https://doi.org/10.1021/acsomega.2c00097
ACS Omega 2022, 7, 11226−11239

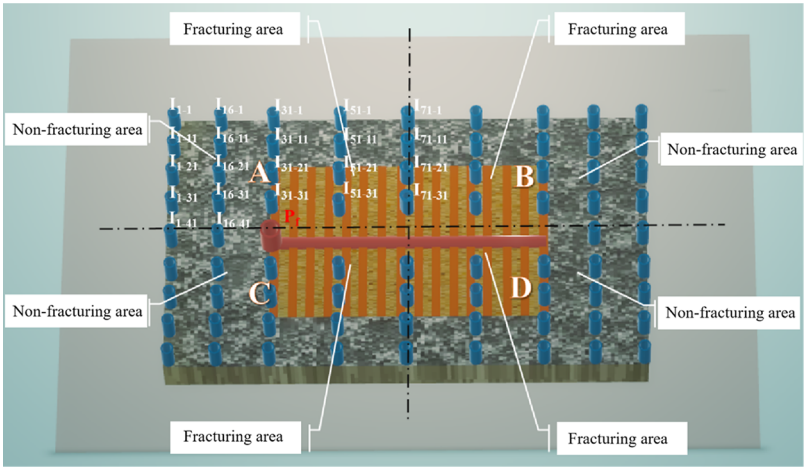

Figure 8. Reservoir model of one-well injection and one-well production horizontal−vertical well pattern.

Table 5. Production Time and Cumulative Oil Production of the Horizontal Well in Different Schemes

scheme	the production time, d	cumulative oil production, m^3	scheme	the production time, d	cumulative oil production, m^3
LX1-1	4430	24164	LX31-11	2220	12,409.64
LX1-11	4160	22,756.62	LX31-21	1180	7410.55
LX1-21	4080	21,886.51	LX31-31	610	4646.06
LX1-31	4050	21,303.44	LX51-1	4420	23,517.91
LX1-41	4090	21,270.68	LX51-11	3170	17,082.34
LX16-1	3800	20,511.72	LX51-21	2030	11,404.94
LX16-11	3110	17,141.04	LX51-31	960	6185.23
LX16-21	2590	14,454.75	LX71-1	5040	26,137.62
LX16-31	2130	11,816.99	LX71-11	3410	18,142.48
LX16-41	2000	10,928.94	LX71-21	2130	11,818.11
LX31-1	3390	18,340.27	LX71-31	970	6232.69

performance and avoid the effect of other injection wells in the horizontal−vertical well pattern, the reservoir model of one-well injection and one-well production is established, as shown in Figure 8. The horizontal well length is 800 m and includes 17 fractures. Besides, other reservoir parameters of the model are the same as those of the inverted five-spot horizontal−vertical well pattern reservoir model.

Region A, B, C, and D in the one-well injection and one-well production model are central symmetry and axial symmetry, so we just need to investigate the influence of the injection well in different positions of region A on the horizontal well production performance. There are 22 relative positions in total in region A, which can be characterized by matrix I. A series of schemes with different injection well positions are conducted while keeping the other parameters the same. Both the production time when the daily oil production rate decreases to 3 m^3/d and the corresponding cumulative oil production are taken to evaluate the influence of the injection well position on the horizontal well production performance.

$$I = \begin{bmatrix} I_{1-1} & I_{16-1} & I_{31-1} & I_{51-1} & I_{71-1} \\ I_{1-11} & I_{16-11} & I_{31-11} & I_{51-11} & I_{71-11} \\ I_{1-21} & I_{16-21} & I_{31-21} & I_{51-21} & I_{71-21} \\ I_{1-31} & I_{16-31} & I_{31-31} & I_{51-31} & I_{71-31} \\ I_{1-41} & I_{16-41} & & & \end{bmatrix} \quad (2)$$

Table 5 shows the production time and cumulative oil production of the horizontal well in different schemes when the daily oil production rate decreases to 3 m^3/d. From Table 5 and matrix I, the cumulative oil production increases with the increase in the distance between the injection well and the horizontal well. To intuitively reflect the influence of the injection well position on the horizontal well production performance, simulation results are interpolated to obtain the plane distribution relationship between the injection well position in region A and the production time and the cumulative oil production, respectively, as shown in Figure 9.

Because region A, B, C, and D are central symmetry and axial symmetry, the plane distribution relationship between the injection well position and the cumulative oil production in the horizontal−vertical well pattern can be obtained. The horizontal−vertical well pattern can be separated into three injection grade regions with spindle shape, as shown in Figure 10. The horizontal well production performance becomes worse with the increase in injection grades. Moreover, when the injection well is in the black region of the horizontal−vertical well pattern, water channeling could be easily caused, so the production performance of the horizontal well is the worst.

4.4.2.2. Control Area of Injection Wells. The influence of injection proportion of injection wells on the performance of asynchronous cyclic waterflooding in the inverted seven-spot horizontal−vertical well pattern indicates that, even if injection wells are in the same injection grade region, the performances of asynchronous cyclic waterflooding varies due to the difference in the control area of injection wells. Therefore, it is necessary to investigate the control area of injection wells in different positions of the horizontal−vertical well pattern. In this section,

https://doi.org/10.1021/acsomega.2c00097
ACS Omega 2022, 7, 11226−11239

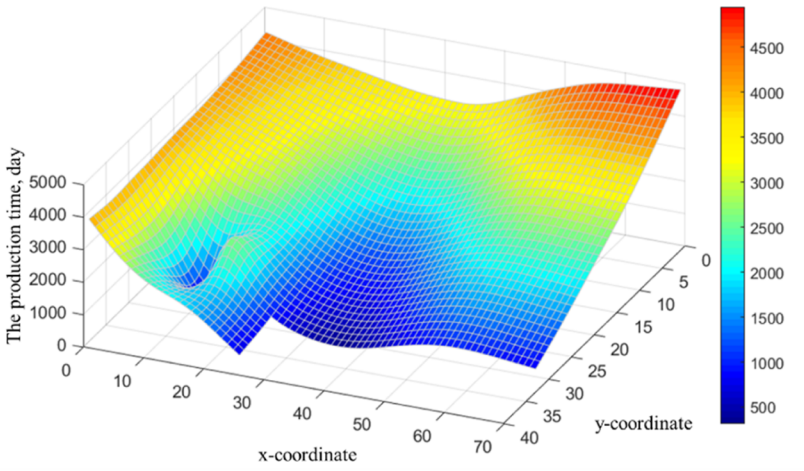

(a)

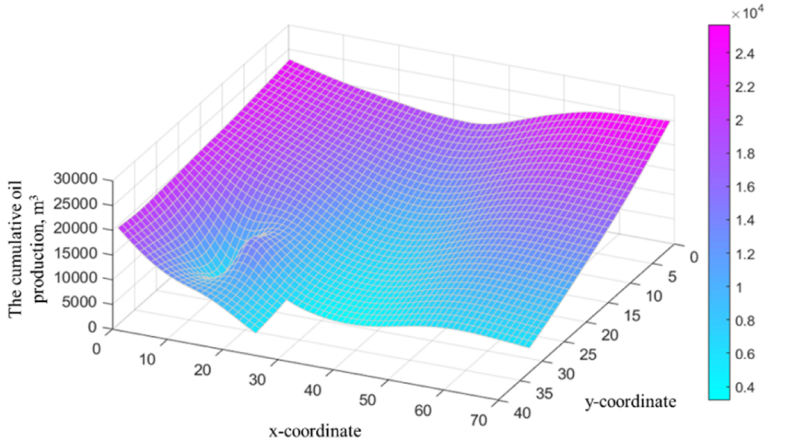

(b)

Figure 9. Plane distribution relationship of the (a) injection well position vs production time and the (b) injection well position vs cumulative oil production.

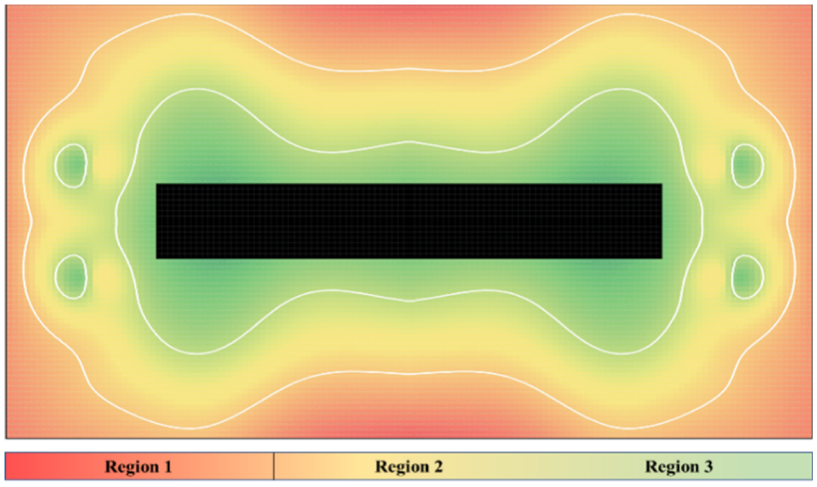

Figure 10. Regional division of injection grades in the horizontal−vertical well pattern.

by determining positions in the horizontal−vertical well pattern, which are controlled by the injection well, the control area of injection wells can be obtained. Darcy's law indicates that the time that the injected water flows into a certain position of the horizontal−vertical well pattern is inversely proportional to the permeability between the injection well and the certain position

https://doi.org/10.1021/acsomega.2c00097
ACS Omega 2022, 7, 11226−11239

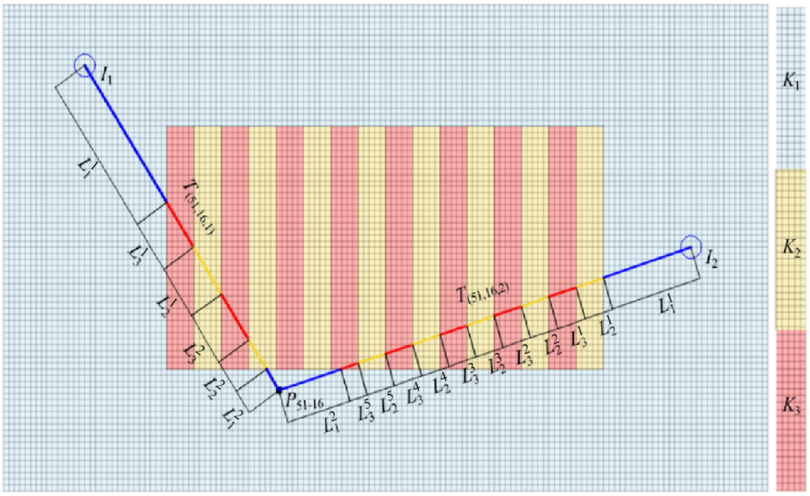

Figure 11. Calculation model of the relative transmit time.

and proportional to the distance between them. Therefore, assuming that injection rates of injection wells in the horizontal−vertical well pattern are the same and the injection wells do not interfere with each other, the ratio of the permeability between the injection well and the certain position to the distance between them is proposed to calculate the relative transmit time. By meshing the horizontal−vertical well pattern and simplifying the main and secondary fracture in the fracturing area, the calculation model of relative transmit time between the injection well and each grid is established, as shown in Figure 11. It can be seen from Figure 11 that the length of the line between the grid P_{i-j} and the injection well I_k in the main fracture area is L_1, in the secondary fracture area is L_2, and in the matrix area is L_3. Therefore, the relative transmit time between the grid P_{i-j} and the injection well I_k can be calculated using eqs 3 and 4

$$t_{(i,j,k)} = \sum_{o=1}^{3} L_o/K_o \tag{3}$$

$$\begin{cases} L_1 = \sum_{i=1}^{m} L_1^i \\ L_2 = \sum_{i=1}^{n} L_2^i \\ L_3 = \sum_{i=1}^{j} L_3^i \end{cases} \tag{4}$$

where K_1, K_2, and K_3 are the permeability in the main fracturing area, the permeability in the secondary fracturing area, and the permeability in the matrix area, respectively. m, n, and j represent the number of the matrix, the number of the main fracturing area, and the number of the secondary fracturing area on the line between the grid P_{i-j} and the injection well I_k.

The relative transmit time set $(t_{(i,j,1)}, t_{(i,j,2)}, t_{(i,j,k)})$ between the grid P_{i-j} and different injection wells (I_1, I_2, and I_k) can be calculated using eqs 3 and 4, and the injection well corresponding to the minimum value of the relative transmit time is defined as the control injection well of the grid P_{i-j}. Given the control area continuity of the same injection well, if one grid is controlled by one injection well, the other injection well cannot control the other grids through the grid. Based on the principle, solving results are corrected, and the control area of each injection well is calculated.

4.4.2.3. Optimization of Injection Proportion. Based on the study above, the injection proportion of injection wells in the horizontal−vertical well pattern can be determined by the fuzzy comprehensive evaluation method.

(1) The determination of index value

From Section 4.4.2.1, the average cumulative oil productions of the horizontal well when injection wells are in region 1, region 2, and region 3, respectively, are shown in Figure 12.

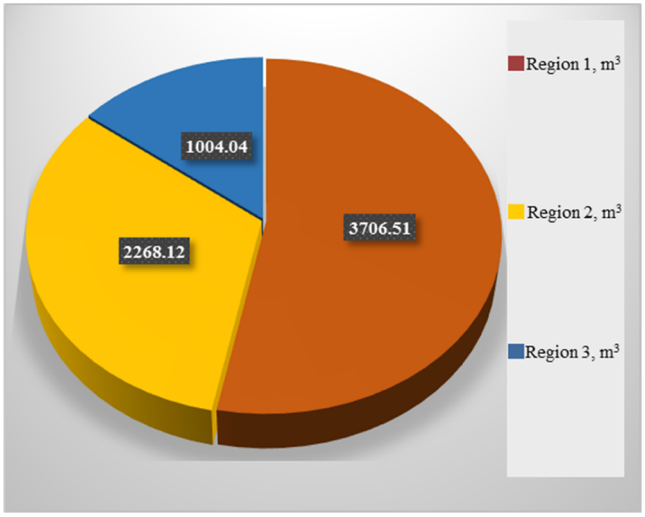

Figure 12. Average cumulative oil production of the horizontal well when injection wells are in region 1, region 2, and region 3.

Furthermore, the index value of injection wells in different injection grade regions (ξ_{R-k}) can be obtained by normalization, where $\xi_{R1-k} = 0.5311$, $\xi_{R2-k} = 0.325$, and $\xi_{R3-k} = 0.1439$. In addition, the control area index of injection wells (ξ_{s-k}) is the ratio of the control area of the injection well to the sum of the control area of each injection well in the horizontal−vertical well pattern.

(2) The establishment of fuzzy comprehensive evaluation model

https://doi.org/10.1021/acsomega.2c00097
ACS Omega 2022, 7, 11226−11239

The attribute weight of the injection well position is assumed to be α, and that of the injection well control area is β. For the horizontal−vertical well pattern with n injection wells (I_1, I_2, ..., I_n), the injection proportion of injection wells I_k can be calculated using eqs 5 and 6.

$$\xi_k = \alpha \cdot \xi_{R-k} / \sum_{k=1}^{F} \xi_{R-k} + \beta \cdot \xi_{s-k} \quad (5)$$

$$\alpha + \beta = 1 \quad (6)$$

To determine the attribute weight, the horizontal−vertical well pattern of three-well injection and one-well production in the Fuxian area of Yanchang oilfield is established, as shown in Figure 13. From Figure 13, the index value of injection wells in

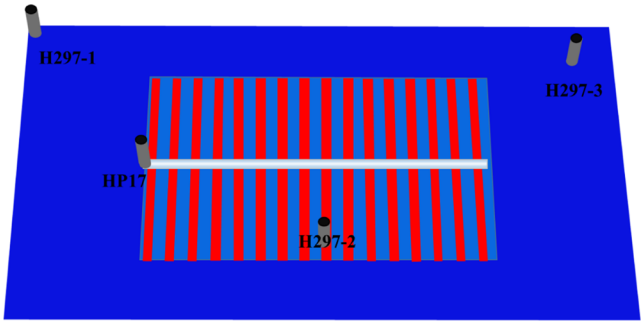

Figure 13. Horizontal−vertical well pattern reservoir model of three-well injection and one-well production.

different injection grade regions (ξ_{R-k}) and the index value of injection well control area (ξ_{s-k}) can be obtained, respectively, as shown in Table 6.

Table 6. Optimization Schemes of α and β

scheme	α	β	$\xi_1(I_1)$	$\xi_2(I_2)$	$\xi_3(I_3)$
1	0.1	0.9	0.12781	0.1315	0.74069
2	0.2	0.8	0.17262	0.153	0.67438
3	0.3	0.7	0.21743	0.1745	0.60807
4	0.4	0.6	0.26224	0.196	0.54176
5	0.5	0.5	0.30705	0.2175	0.47545
6	0.6	0.4	0.35186	0.239	0.40914
7	0.7	0.3	0.39667	0.2605	0.34283
8	0.8	0.2	0.44148	0.29652	0.262
9	0.9	0.1	0.48629	0.3035	0.21021
10			1/3	1/3	1/3

Nine schemes are designed with different α, ranging from 0.1 to 0.9, the corresponding β can be determined by $\alpha + \beta = 1$. Moreover, a control scheme with the same injection proportion is added. Schemes are shown in Table 6.

Based on the horizontal well oil production of Scheme 10, simulation results of the remaining nine schemes are standardized and shown in Figure 14. From Figure 14, Scheme 8 obtains the best production performance, and the corresponding attribute weights of α and β are 0.8 and 0.2, respectively. Besides, when $\beta > \alpha$, the development effect of schemes is worse than that of control Scheme 9, which means that the injection well position has a more significant influence on the horizontal well production performance of asynchronous cyclic waterflooding than the control area of injection wells. To verify the accuracy of the optimal attribute weight ($\alpha = 0.8$ and $\beta = 0.2$), the injection proportion of corner wells and edge wells in the inverted seven-spot horizontal−vertical well pattern, calculated based on the optimal attribute weight, are compared with those corresponding to the optimal development scheme in Section 4.4.1. The result shows that the error between the injection proportion of corner wells and edge wells calculated based on the attribute weight $\alpha = 0.8$ and $\beta = 0.2$ and those of the optimal development scheme is less than 5%. Therefore, the optimal attribute weight $\alpha = 0.8$ and $\beta = 0.2$ can provide some guidance for the determination of the injection proportion of injection wells in the horizontal−vertical well pattern for asynchronous cyclic waterflooding.

5. OILFIELD TEST

Yanchang oilfield is abundant in tight oil resources, and the tight reservoir of Chang8 formation in the Fuxian area plays a significant role in the tight oil resource of Yanchang oilfield. Huangjialing block in the Fuxian area is located in the southeast of the Ordos Basin, NW China and presents a gentle western-leaning monoclinal structure, as shown in Figure 15a, which is the typical representative of the tight oil reservoir in the Triassic Yanchang Formation in the Ordos Basin. The average porosity of Chang8 formation in the Huangjialing block is 7.65%, and the average permeability is 0.17 mD. To further verify the accuracy of the parameter optimization for the horizontal−vertical well pattern, the optimization result was practically applied on the horizontal well (HP17) in the Huangjialing block (Figure 15b). HP297-1 is a well row, HP297-2 and HP297-3 are another well row, the injection time interval is 46 days, and the injection and shut-in time are both 92 days. In addition, the injection proportions of H297-1, HP297-2, and HP297-3 are 0.49, 0.21, and 0.3, respectively, and the injection−production ratio is 1. After the implementation of asynchronous cyclic waterflooding, the average daily oil production of HP17 increased from 1.7 to 3 m^3, which is close to twice that before the implementation of asynchronous cyclic waterflooding. Besides, the average water cut also declined slightly, from 68 to 64.6%. Those proved that asynchronous cyclic waterflooding can not only increase the swept area of waterflooding but also reduce the water cut of horizontal wells to a certain extent, which further verifies the efficiency of the parameter optimization for the horizontal−vertical well pattern.

6. CONCLUSIONS

1. The main oil recovery mechanisms of asynchronous cyclic waterflooding in the horizontal−vertical well pattern are the pressure disturbance and the streamline deviation, which can expand the swept area of injected water and improve the oil recovery of waterflooding.
2. The influence of the asynchronous mode on the performance of asynchronous cyclic waterflooding can be summarized as follows: $W_{AD} > W_{AS} > W_{AL} > W_{AC}$, and the optimal asynchronous mode is W_{AD}. With the increase in injection time interval and injection−production ratio, the cumulative oil production increases first and then declines; the optimal injection time interval is 0.5 T, and the optimal injection−production ratio is around 1. With the increase in injection and shut-in time, the cumulative oil production shows a trend of increasing first and then decreasing. The optimal injection and shut-in time can be determined by the empirical formula. The influence of injection proportion on the performance of asynchronous

https://doi.org/10.1021/acsomega.2c00097
ACS Omega 2022, 7, 11226−11239

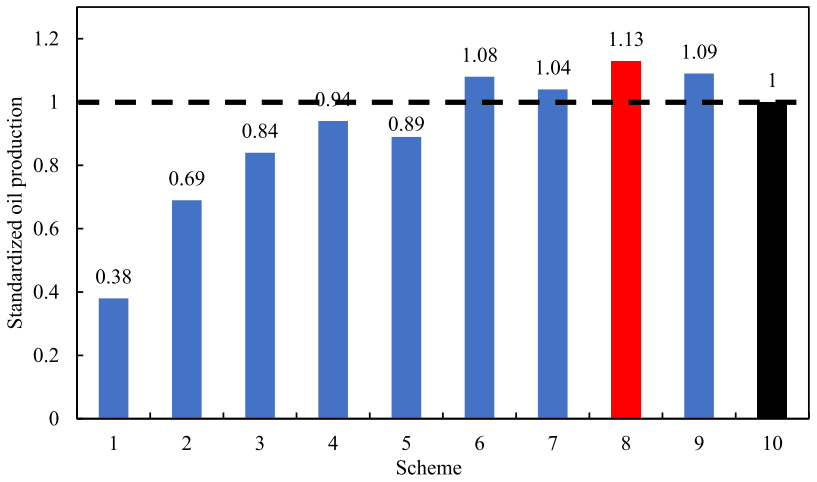

Figure 14. Simulation results of attribute weight optimization.

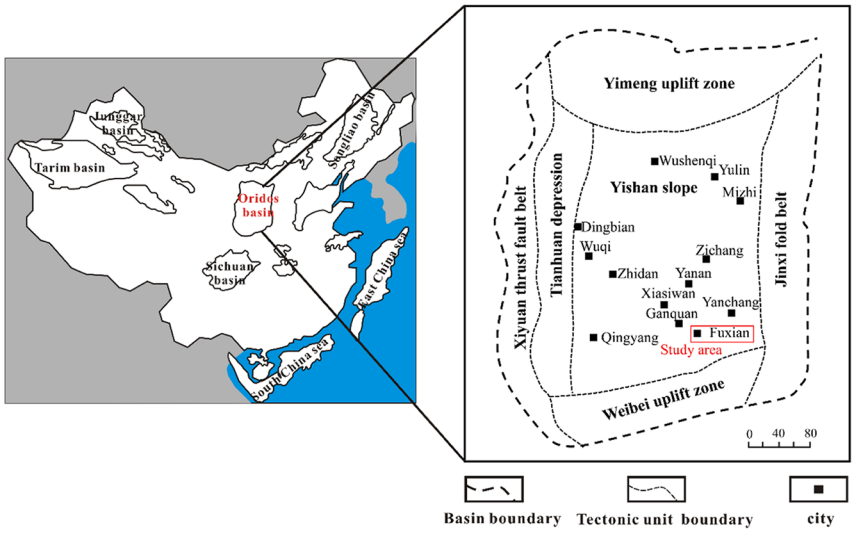

(a)

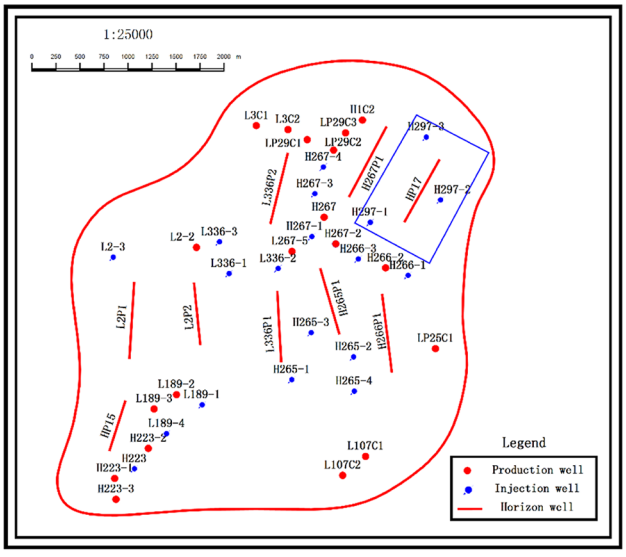

(b)

Figure 15. (a) Location of the study area. (b) Distribution of the well location.

https://doi.org/10.1021/acsomega.2c00097
ACS Omega 2022, 7, 11226−11239

cyclic waterflooding can be concluded as follows: the scheme of classified balanced injection proportion > the scheme of generally balanced injection proportion > and the scheme of casual injection proportion. The classified balanced injection scheme is more beneficial to asynchronous cyclic waterflooding.

3. The horizontal−vertical well pattern can be divided into three spindle-shaped injection grade regions, and the performance of asynchronous cyclic waterflooding becomes worse with the increase in the injection grade. Besides, the control area of injection wells can be calculated by the calculation model of the relative transmit time. On this foundation, the injection proportion of injection wells is ultimately determined by the fuzzy synthetic evaluation method, in which the optimal weight values of the injection well position and the control area of injection wells are 0.8 and 0.2, respectively.
4. Field practices showed that the average daily oil production after the implementation of asynchronous cyclic waterflooding was increased from 1.7 to 3.5 m^3, and the water cut was reduced to some extent, which not only verify the efficiency of the optimized parameters but also highlight the great potential of asynchronous cyclic waterflooding in enhancing oil production.

AUTHOR INFORMATION

Corresponding Author

Chunsheng Pu − *School of Petroleum Engineering, China University of Petroleum (East China), Qingdao, Shandong 266555, China*; orcid.org/0000-0002-0724-5591; Email: chshpu_tx@126.com

Authors

Shaofei Kang − *School of Petroleum Engineering, China University of Petroleum (East China), Qingdao, Shandong 266555, China*

Yuchuan Wang − *China United Coalbed Methane Corporation Ltd, Taiyuan, Shanxi 030000, China*

Wei Liu − *China Petroloil Production Plant No. 7 Changqing Oilfield Company, Huan County, Gansu 745700, China*

Kai Wang − *School of Petroleum Engineering, China University of Petroleum (East China), Qingdao, Shandong 266555, China*

Feifei Huang − *School of Petroleum Engineering, Yan'an University, Yanan, Shaanxi 716000, China*

Qiao Fan − *School of Petroleum Engineering, China University of Petroleum (East China), Qingdao, Shandong 266555, China*

Xiang Gao − *School of Petroleum Engineering, China University of Petroleum (East China), Qingdao, Shandong 266555, China*

Qiangqiang Yang − *Yanchang Petroleum Group Exploration Company, Yanan, Shaanxi 716000, China*

Complete contact information is available at: https://pubs.acs.org/10.1021/acsomega.2c00097

Notes

The authors declare no competing financial interest.

ACKNOWLEDGMENTS

This research was supported by the National Natural Science Foundation of China (grant number 51904320). The authors also appreciate the financial support from Jing Liu for the study of this paper.

REFERENCES

(1) Wang, X.; Peng, X.; Zhang, S.; Du, Z.; Zeng, F. Characteristics of oil distributions in forced and spontaneous imbibition of tight oil reservoir. *Fuel* **2018**, *224*, 280−288.

(2) Zhou, X.; Yuan, Q.; Zhang, Y.; Wang, H.; Zeng, F.; Zhang, L. Performance evaluation of CO2 flooding process in tight oil reservoir via experimental and numerical simulation studies. *Fuel* **2019**, *236*, 730−746.

(3) McGlade, C. E. A review of the uncertainties in estimates of global oil resources. *Energy* **2012**, *47*, 262−270.

(4) Zou, C.; Zhu, R.; Wu, S.; Yang, Z.; Tao, S.; Yuan, X.; Hou, L.; Yang, H.; Xu, C.; Li, D. Types, characteristics, genesis and prospects of conventional and unconventional hydrocarbon accumulations: taking tight oil and tight gas in China as an instance. *Acta Pet. Sin.* **2012**, *33*, 173−187.

(5) Zou, C.; Zhang, G.; Yang, Z.; Tao, S.; Hou, L.; Zhu, R.; Yuan, X.; Ran, Q.; Li, D.; Wang, Z. Geological concepts, characteristics, resource potential and key techniques of unconventional hydrocarbon: On unconventional petroleum geology. *Pet. Explor. Dev.* **2013**, *40*, 385−399.

(6) Jia, C.; Zheng, M.; Zhang, Y. Unconventional hydrocarbon resources in China and the prospect of exploration and development. *Pet. Explor. Dev.* **2012**, *39*, 139−146.

(7) Sun, L.; Zou, C.; Jia, A.; Wei, Y.; Zhu, R.; Wu, S.; Guo, Z. Development characteristics and orientation of tight oil and gas in China. *Pet. Explor. Dev.* **2019**, *46*, 1073−1087.

(8) Hu, J.; Sun, R.; Zhang, Y. Investigating the horizontal well performance under the combination of micro-fractures and dynamic capillary pressure in tight oil reservoirs. *Fuel* **2020**, *269*, 117375.

(9) Wu, F.; Li, D.; Fan, X.; Liu, J.; Li, X. Analytical interpretation of hydraulic fracturing initiation pressure and breakdown pressure. *J. Nat. Gas Sci. Eng.* **2020**, *76*, 103185.

(10) Siddhamshetty, P.; Wu, K.; Kwon, J. S.-I. Modeling and control of proppant distribution of multistage hydraulic fracturing in horizontal shale wells. *Ind. Eng. Chem. Res.* **2019**, *58*, 3159−3169.

(11) Hu, J.-H.; Zhao, J.-Z.; Li, Y.-M. A proppant mechanical model in postfrac flowback treatment. *J. Nat. Gas Sci. Eng.* **2014**, *20*, 23−26.

(12) Chang, Y.; Lu, H.; Chen, B.; Ji, Z.; Wang, C.; Qi, Y.; Li, J. S.; Du, X.; Yin, G. Multi-fracture stimulation techniques make better wells in ultra-low permeability oil reservoirs. *Unconventional Resources Technology Conference*, Denver, Colorado, August 12−14, 2013.

(13) Zhao, J.; Fan, J.; He, Y.; Yang, Z.; Gao, W.; Gao, W. Optimization of horizontal well injection-production parameters for ultra-low permeable−tight oil production: a case from Changqing Oilfield, Ordos Basin, NW China. *Pet. Explor. Dev.* **2015**, *42*, 74−82.

(14) Wang, J.; Liu, J.; Li, Z.; Li, H.; Zhang, J.; Li, W.; Zhang, Y.; Ping, Y.; Yang, H.; Wang, P. Synchronous injection-production energy replenishment for a horizontal well in an ultra-low permeability sandstone reservoir: A case study of Changqing oilfield in Ordos Basin, NW China. *Pet. Explor. Dev.* **2020**, *47*, 827−835.

(15) Todd, H. B.; Evans, J. G. Improved oil recovery IOR pilot projects in the Bakken formation. *SPE Low Perm Symposium*; OnePetro, 2016.

(16) Qin, G.; Dai, X.; Sui, L.; Geng, M.; Sun, L.; Zheng, Y.; Bai, Y. Study of massive water huff-n-puff technique in tight oil field and its field application. *J. Pet. Sci. Eng.* **2021**, *196*, 107514.

(17) Yu, Y.; Sheng, J. J. A comparative experimental study of IOR potential in fractured shale reservoirs by cyclic water and nitrogen gas injection. *J. Pet. Sci. Eng.* **2017**, *149*, 844−850.

(18) Kanfar, M.; Clarkson, C. Factors affecting huff-n-puff efficiency in hydraulically-fractured tight reservoirs. *SPE Unconventional Resources Conference*, Calgary, Alberta, February 15−16, 2017.

(19) Chen, T.; Yang, Z.; Ding, Y.; Luo, Y.; Qi, D.; Lin, W.; Zhao, X. Waterflooding huff-n-puff in tight oil cores using online nuclear magnetic resonance. *Energies* **2018**, *11*, 1524.

(20) Loahardjo, N.; Xie, X.; Morrow, N. R. Oil recovery by sequential waterflooding of mixed-wet sandstone and limestone. *Energy Fuels* **2010**, *24*, 5073−5080.
(21) Jianming, F.; Wang, C.; Qu, X.; Cheng, L.; Xue, T. Development and practice of water flooding huff-puff in tight oil horizontal well, Ordos Basin: A case study of Yanchang Formation Chang 7 oil layer. *Acta Pet. Sin.* **2019**, *40*, 706−715.
(22) Janiga, D.; Czarnota, R.; Stopa, J.; Wojnarowski, P. Huff and puff process optimization in micro scale by coupling laboratory experiment and numerical simulation. *Fuel* **2018**, *224*, 289−301.
(23) Popa, C.; Clipea, M. Improved waterflooding efficiency by horizontal wells. *SPE International Conference on Horizontal Well Technology*, Alberta, Canada, November 1−4, 1998.
(24) Xu, Q.; Guan, R.; Wu, C. Comparison of Development Effects for Two Different Combined Well Patterns with Horizontal Wells and Vertical Wells. *Proceedings of the International Field Exploration and Development Conference*; Springer: Singapore, 2019; pp 244−248.
(25) Qu, D.; Ge, J.; Wang, D. Combination production of vertical and horizontal wells−5-spot well pattern. *Pet. Explor. Dev.* **1995**, *1*, 35−38+8586.
(26) Lang, Z.; Zhang, H.; Chen, L.; Li, C. Combined production of vertical and horizontal wells—A 5-spot well pattern. *J. Univ. Pet.* **1993**, *17*, 50−55. [in Chinese]
(27) Ge, J.; Wang, D.; Qu, D. A combination of vertical and horizontal wells, in a 7-spot well pattern [J]. *Pet. Explor. Dev.* **1995**, *2*, 47−50+100.
(28) Wu, B.; Yao, J.; Zhang, J.; Lu, A. Determination of water breakthrough time in horizontal-vertical well pattern. *Acta Pet. Sin.* **2005**, *26*, 111−114.
(29) Wu, B.; Yao, J.; Lu, A. Research on sweep efficiency in horizontal-vertical combined well pattern. *Acta Pet. Sin.* **2006**, *4*, 85−88.
(30) Surguchev, L.; Koundin, A.; Melberg, O.; Rolfsvåg, T. A.; Menard, W. P. Cyclic water injection: improved oil recovery at zero cost. *Pet. Geosci.* **2002**, *8*, 89−95.
(31) Shchipanov, A.; Surguchev, L.; Jakobsen, S. Improved oil recovery by cyclic injection and production. *SPE Russian Oil and Gas Technical Conference and Exhibition*, Moscow, Russia, October 28-30, 2008.
(32) Yanzhang, H.; Shang, G.; Chen, Y. A study on the mechanisms of cyclic water floodiing by nmri techniques. *Acta Pet. Sin.* **1995**, *4*, 62−67.
(33) Yang, Y.; Dai, T.; Wang, C. The reservoir simulation research and extending application about cyclic water injection. *International Oil & Gas Conference and Exhibition in China*, Beijing, China, December 5, 2006.
(34) Surguchev, L. M.; Giske, N. H.; Kollbotn, L.; Shchipanov, A. Cyclic water injection improves oil production in carbonate reservoir. *Abu Dhabi International Petroleum Exhibition and Conference*, Abu Dhabi, UAE, November 3−6, 2008.
(35) Montaron, B. A.; Bradley, D. C.; Cooke, A.; Prouvost, L. P.; Raffn, A. G.; Vidal, A.; Wilt, M. Shapes of flood fronts in heterogeneous reservoirs and oil recovery strategies. *SPE/EAGE Reservoir Characterization and Simulation Conference*, Abu Dhabi, UAE, October 28−31, 2007.
(36) He, Y.; Cheng, S.; Li, L.; Mu, G.; Zhang, T.; Xu, H.; Qin, J.; Yu, H. Waterflood direction and front characterization with four-step work flow: a case study in changqing oil field China. *SPE Reservoir Eval. Eng.* **2017**, *20*, 708−725.
(37) Meng, X.; Zhang, Q.; Dai, X.; Xue, S.; Feng, X.; Zhang, Y.; Tu, B.; Li, X. Experimental and simulation investigations of cyclic water injection in low-permeability reservoir. *Arabian J. Geosci.* **2021**, *14*, 791.
(38) Qi-tai, Y.; Zhang, S. A second report on the study for the cyclic flooding by numerical reservoir simulation. *Pet. Explor. Dev.* **1994**, *21*, 56−61.
(39) Sun, X.; Zhang, Y.; Wu, J.; Xie, M.; Hu, H. Optimized Cyclic Water Injection Strategy for Oil Recovery in Low-Permeability Reservoirs. *J. Energy Resour. Technol.* **2019**, *141*, 012905.
(40) Pourabdollah, K. Process design of cyclic water flooding by real-time monitoring. *J. Energy Resour. Technol.* **2018**, *140*, 112701.
(41) Yu, Q.; Zhang, S. A preliminary report of the numerical reservoir simulation study for the cyclic flooding. *Pet. Explor. Dev.* **1993**, *6*, 46−53.
(42) Zhang, J.; Bai, S.; Zhang, Y.; Ban, Y. Cyclic water flooding experiments and research on mechanism of enhancing oil production. *Acta Pet. Sin.* **2003**, *24*, 76−80.
(43) Wang, X.; Wang, J.; Wang, D.; Ning, L.; Gong, Y. Study on cyclic water injection test in Gasikule Oilfield. *Special Oil Gas Reservoirs* **2005**, *06*, 50−52+106.

https://doi.org/10.1021/acsomega.2c00097
ACS Omega 2022, 7, 11226−11239